MIT Libraries | DSpace@MIT

MIT Open Access Articles

Measurement of the top quark mass in the all-hadronic mode at CDF

Massachusetts Institute of Technology

Measurement of the top quark mass in the all-hadronic mode at CDF

CDF Collaboration

T. Aaltonen [w], B. Álvarez González [j,27], S. Amerio [ax], D. Amidei [ap], A. Anastassov [q,25], A. Annovi [s], J. Antos [m,n], G. Apollinari [q], J.A. Appel [q], T. Arisawa [br], A. Artikov [o], J. Asaadi [bl], W. Ashmanskas [q], B. Auerbach [bu], A. Aurisano [bl], F. Azfar [aw], W. Badgett [q], T. Bae [aa,ab,ac,ad,ae,af], A. Barbaro-Galtieri [ag], V.E. Barnes [bf], B.A. Barnett [y], P. Barria [bc,ba], P. Bartos [m,n], M. Bauce [ay,ax], F. Bedeschi [ba], S. Behari [y], G. Bellettini [bb,ba], J. Bellinger [bt], D. Benjamin [p], A. Beretvas [q], A. Bhatti [bh], D. Bisello [ay,ax], I. Bizjak [ai], K.R. Bland [e], B. Blumenfeld [y], A. Bocci [p], A. Bodek [bg], D. Bortoletto [bf], J. Boudreau [be], A. Boveia [l], L. Brigliadori [g,f,*], C. Bromberg [aq], E. Brucken [w], J. Budagov [o], H.S. Budd [bg], K. Burkett [q], G. Busetto [ay,ax], P. Bussey [u], A. Buzatu [al,am,an,ao], A. Calamba [k], C. Calancha [aj], S. Camarda [d], M. Campanelli [ai], M. Campbell [ap], F. Canelli [l,q], B. Carls [x], D. Carlsmith [bt], R. Carosi [ba], S. Carrillo [r,14], S. Carron [q], B. Casal [j,12], M. Casarsa [bm], A. Castro [g,f], P. Catastini [v], D. Cauz [bm], V. Cavaliere [x], M. Cavalli-Sforza [d], A. Cerri [ag,7], L. Cerrito [ai,20], Y.C. Chen [a], M. Chertok [h], G. Chiarelli [ba], G. Chlachidze [q], F. Chlebana [q], K. Cho [aa,ab,ac,ad,ae,af], D. Chokheli [o], W.H. Chung [bt], Y.S. Chung [bg], M.A. Ciocci [bc,ba], A. Clark [t], C. Clarke [bs], G. Compostella [ay,ax], M.E. Convery [q], J. Conway [h], M. Corbo [q], M. Cordelli [s], C.A. Cox [h], D.J. Cox [h], F. Crescioli [bb,ba], J. Cuevas [j,27], R. Culbertson [q], D. Dagenhart [q], N. d'Ascenzo [q,24], M. Datta [q], P. de Barbaro [bg], M. Dell'Orso [bb,ba], L. Demortier [bh], M. Deninno [f], F. Devoto [w], M. d'Errico [ay,ax], A. Di Canto [bb,ba], B. Di Ruzza [q], J.R. Dittmann [e], M. D'Onofrio [ah], S. Donati [bb,ba], P. Dong [q], M. Dorigo [bm], T. Dorigo [ax], K. Ebina [br], A. Elagin [bl], A. Eppig [ap], R. Erbacher [h], S. Errede [x], N. Ershaidat [q,31], R. Eusebi [bl], S. Farrington [aw], M. Feindt [z], J.P. Fernandez [aj], R. Field [r], G. Flanagan [q,22], R. Forrest [h], M.J. Frank [e], M. Franklin [v], J.C. Freeman [q], Y. Funakoshi [br], I. Furic [r], M. Gallinaro [bh], J.E. Garcia [t], A.F. Garfinkel [bf], P. Garosi [bc,ba], H. Gerberich [x], E. Gerchtein [q], S. Giagu [bi], V. Giakoumopoulou [c], P. Giannetti [ba], K. Gibson [be], C.M. Ginsburg [q], N. Giokaris [c], P. Giromini [s], G. Giurgiu [y], V. Glagolev [o], D. Glenzinski [q], M. Gold [as], D. Goldin [bl], N. Goldschmidt [r], A. Golossanov [q], G. Gomez [j], G. Gomez-Ceballos [ak], M. Goncharov [ak], O. González [aj], I. Gorelov [as], A.T. Goshaw [p], K. Goulianos [bh], S. Grinstein [d], C. Grosso-Pilcher [l], R.C. Group [bq,q], J. Guimaraes da Costa [v], S.R. Hahn [q], E. Halkiadakis [bk], A. Hamaguchi [av], J.Y. Han [bg], F. Happacher [s], K. Hara [bo], D. Hare [bk], M. Hare [bp], R.F. Harr [bs], K. Hatakeyama [e], C. Hays [aw], M. Heck [z], J. Heinrich [az], M. Herndon [bt], S. Hewamanage [e], A. Hocker [q], W. Hopkins [q,8], D. Horn [z], S. Hou [a], R.E. Hughes [at], M. Hurwitz [l], U. Husemann [bu], N. Hussain [al,am,an,ao], M. Hussein [aq], J. Huston [aq], G. Introzzi [ba], M. Iori [bj,bi], A. Ivanov [h,17], E. James [q], D. Jang [k], B. Jayatilaka [p], E.J. Jeon [aa,ab,ac,ad,ae,af], S. Jindariani [q], M. Jones [bf], K.K. Joo [aa,ab,ac,ad,ae,af], S.Y. Jun [k], T.R. Junk [q], T. Kamon [aa,ab,ac,ad,ae,af,bl], P.E. Karchin [bs], A. Kasmi [e], Y. Kato [av,16], W. Ketchum [l], J. Keung [az], V. Khotilovich [bl], B. Kilminster [q], D.H. Kim [aa,ab,ac,ad,ae,af], H.S. Kim [aa,ab,ac,ad,ae,af], J.E. Kim [aa,ab,ac,ad,ae,af], M.J. Kim [s], S.B. Kim [aa,ab,ac,ad,ae,af], S.H. Kim [bo], Y.K. Kim [l], Y.J. Kim [aa,ab,ac,ad,ae,af], N. Kimura [br], M. Kirby [q], S. Klimenko [r], K. Knoepfel [q], K. Kondo [br,1], D.J. Kong [aa,ab,ac,ad,ae,af], J. Konigsberg [r], A.V. Kotwal [p], M. Kreps [z], J. Kroll [az], D. Krop [l], M. Kruse [p], V. Krutelyov [bl,4], T. Kuhr [z], M. Kurata [bo], S. Kwang [l], A.T. Laasanen [bf], S. Lami [ba], S. Lammel [q], M. Lancaster [ai], R.L. Lander [h], K. Lannon [at,26], A. Lath [bk], G. Latino [bc,ba], T. LeCompte [b], E. Lee [bl], H.S. Lee [l,18], J.S. Lee [aa,ab,ac,ad,ae,af], S.W. Lee [bl,29], S. Leo [bb,ba],

* Corresponding author.
  E-mail address: Luca.Brigliadori@bo.infn.it (L. Brigliadori).

S. Leone [ba], J.D. Lewis [q], A. Limosani [p,21], C.-J. Lin [ag], M. Lindgren [q], E. Lipeles [az], A. Lister [t],
D.O. Litvintsev [q], C. Liu [be], H. Liu [bq], Q. Liu [bf], T. Liu [q], S. Lockwitz [bu], A. Loginov [bu], D. Lucchesi [ay,ax],
J. Lueck [z], P. Lujan [ag], P. Lukens [q], G. Lungu [bh], J. Lys [ag], R. Lysak [m,n,6], R. Madrak [q], K. Maeshima [q],
P. Maestro [bc,ba], S. Malik [bh], G. Manca [ah,2], A. Manousakis-Katsikakis [c], F. Margaroli [bi], C. Marino [z],
M. Martínez [d], P. Mastrandrea [bi], K. Matera [x], M.E. Mattson [bs], A. Mazzacane [q], P. Mazzanti [f],
K.S. McFarland [bg], P. McIntyre [bl], R. McNulty [ah,11], A. Mehta [ah], P. Mehtala [w], C. Mesropian [bh],
T. Miao [q], D. Mietlicki [ap], A. Mitra [a], H. Miyake [bo], S. Moed [q], N. Moggi [f], M.N. Mondragon [q,14],
C.S. Moon [aa,ab,ac,ad,ae,af], R. Moore [q], M.J. Morello [bd,ba], J. Morlock [z], P. Movilla Fernandez [q],
A. Mukherjee [q], Th. Muller [z], P. Murat [q], M. Mussini [g,f], J. Nachtman [q,15], Y. Nagai [bo], J. Naganoma [br],
I. Nakano [au], A. Napier [bp], J. Nett [bl], C. Neu [bq], M.S. Neubauer [x], J. Nielsen [ag,5], L. Nodulman [b],
S.Y. Noh [aa,ab,ac,ad,ae,af], O. Norniella [x], L. Oakes [aw], S.H. Oh [p], Y.D. Oh [aa,ab,ac,ad,ae,af], I. Oksuzian [bq],
T. Okusawa [av], R. Orava [w], L. Ortolan [d], S. Pagan Griso [ay,ax], C. Pagliarone [bm], E. Palencia [j,7],
V. Papadimitriou [q], A.A. Paramonov [b], J. Patrick [q], G. Pauletta [bn,bm], M. Paulini [k], C. Paus [ak], D.E. Pellett [h],
A. Penzo [bm], T.J. Phillips [p], G. Piacentino [ba], E. Pianori [az], J. Pilot [at], K. Pitts [x], C. Plager [i], L. Pondrom [bt],
S. Poprocki [q,8], K. Potamianos [bf], F. Prokoshin [o,30], A. Pranko [ag], F. Ptohos [s,9], G. Punzi [bb,ba], A. Rahaman [be],
V. Ramakrishnan [bt], N. Ranjan [bf], I. Redondo [aj], P. Renton [aw], M. Rescigno [bi], T. Riddick [ai], F. Rimondi [g,f],
L. Ristori [ba,q], A. Robson [u], T. Rodrigo [j], T. Rodriguez [az], E. Rogers [x], S. Rolli [bp,10], R. Roser [q], F. Ruffini [bc,ba],
A. Ruiz [j], J. Russ [k], V. Rusu [q], A. Safonov [bl], W.K. Sakumoto [bg], Y. Sakurai [br], L. Santi [bn,bm], K. Sato [bo],
V. Saveliev [q,24], A. Savoy-Navarro [q,28], P. Schlabach [q], A. Schmidt [z], E.E. Schmidt [q], T. Schwarz [q],
L. Scodellaro [j], A. Scribano [bc,ba], F. Scuri [ba], S. Seidel [as], Y. Seiya [av], A. Semenov [o], F. Sforza [bc,ba],
S.Z. Shalhout [h], T. Shears [ah], P.F. Shepard [be], M. Shimojima [bo,23], M. Shochet [l], I. Shreyber-Tecker [ar],
A. Simonenko [o], P. Sinervo [al,am,an,ao], K. Sliwa [bp], J.R. Smith [h], F.D. Snider [q], A. Soha [q], V. Sorin [d], H. Song [be],
P. Squillacioti [bc,ba], M. Stancari [q], R. St. Denis [u], B. Stelzer [al,am,an,ao], O. Stelzer-Chilton [al,am,an,ao],
D. Stentz [q,25], J. Strologas [as], G.L. Strycker [ap], Y. Sudo [bo], A. Sukhanov [q], I. Suslov [o], K. Takemasa [bo],
Y. Takeuchi [bo], J. Tang [l], M. Tecchio [ap], P.K. Teng [a], J. Thom [q,8], J. Thome [k], G.A. Thompson [x], E. Thomson [az],
D. Toback [bl], S. Tokar [m,n], K. Tollefson [aq], T. Tomura [bo], D. Tonelli [q], S. Torre [s], D. Torretta [q], P. Totaro [ax],
M. Trovato [bd,ba], F. Ukegawa [bo], S. Uozumi [aa,ab,ac,ad,ae,af], A. Varganov [ap], F. Vázquez [r,14], G. Velev [q],
C. Vellidis [q], M. Vidal [bf], I. Vila [j], R. Vilar [j], J. Vizán [j], M. Vogel [as], G. Volpi [s], P. Wagner [az], R.L. Wagner [q],
T. Wakisaka [av], R. Wallny [i], S.M. Wang [a], A. Warburton [al,am,an,ao], D. Waters [ai], W.C. Wester III [q],
D. Whiteson [az,3], A.B. Wicklund [b], E. Wicklund [q], S. Wilbur [l], F. Wick [z], H.H. Williams [az], J.S. Wilson [at],
P. Wilson [q], B.L. Winer [at], P. Wittich [q,8], S. Wolbers [q], H. Wolfe [at], T. Wright [ap], X. Wu [t], Z. Wu [e],
K. Yamamoto [av], D. Yamato [av], T. Yang [q], U.K. Yang [l,19], Y.C. Yang [aa,ab,ac,ad,ae,af], W.-M. Yao [ag], G.P. Yeh [q],
K. Yi [q,15], J. Yoh [q], K. Yorita [br], T. Yoshida [av,13], G.B. Yu [p], I. Yu [aa,ab,ac,ad,ae,af], S.S. Yu [q], J.C. Yun [q],
A. Zanetti [bm], Y. Zeng [p], C. Zhou [p], S. Zucchelli [g,f]

[a] *Institute of Physics, Academia Sinica, Taipei, Taiwan 11529, ROC*
[b] *Argonne National Laboratory, Argonne, IL 60439, USA*
[c] *University of Athens, 157 71 Athens, Greece*
[d] *Institut de Fisica d'Altes Energies, ICREA, Universitat Autonoma de Barcelona, E-08193, Bellaterra (Barcelona), Spain*
[e] *Baylor University, Waco, TX 76798, USA*
[f] *Istituto Nazionale di Fisica Nucleare, Bologna, Italy*
[g] *University of Bologna, I-40127 Bologna, Italy*
[h] *University of California, Davis, Davis, CA 95616, USA*
[i] *University of California, Los Angeles, Los Angeles, CA 90024, USA*
[j] *Instituto de Fisica de Cantabria, CSIC-University of Cantabria, 39005 Santander, Spain*
[k] *Carnegie Mellon University, Pittsburgh, PA 15213, USA*
[l] *Enrico Fermi Institute, University of Chicago, Chicago, IL 60637, USA*
[m] *Comenius University, 842 48 Bratislava, Slovakia*
[n] *Institute of Experimental Physics, 040 01 Kosice, Slovakia*
[o] *Joint Institute for Nuclear Research, RU-141980 Dubna, Russia*
[p] *Duke University, Durham, NC 27708, USA*
[q] *Fermi National Accelerator Laboratory, Batavia, IL 60510, USA*
[r] *University of Florida, Gainesville, FL 32611, USA*
[s] *Laboratori Nazionali di Frascati, Istituto Nazionale di Fisica Nucleare, I-00044 Frascati, Italy*
[t] *University of Geneva, CH-1211 Geneva 4, Switzerland*
[u] *Glasgow University, Glasgow G12 8QQ, United Kingdom*
[v] *Harvard University, Cambridge, MA 02138, USA*
[w] *Division of High Energy Physics, Department of Physics, University of Helsinki and Helsinki Institute of Physics, FIN-00014, Helsinki, Finland*
[x] *University of Illinois, Urbana, IL 61801, USA*
[y] *The Johns Hopkins University, Baltimore, MD 21218, USA*
[z] *Institut für Experimentelle Kernphysik, Karlsruhe Institute of Technology, D-76131 Karlsruhe, Germany*
[aa] *Center for High Energy Physics: Kyungpook National University, Daegu 702-701, Republic of Korea*

[ab] *Seoul National University, Seoul 151-742, Republic of Korea*
[ac] *Sungkyunkwan University, Suwon 440-746, Republic of Korea*
[ad] *Korea Institute of Science and Technology Information, Daejeon 305-806, Republic of Korea*
[ae] *Chonnam National University, Gwangju 500-757, Republic of Korea*
[af] *Chonbuk National University, Jeonju 561-756, Republic of Korea*
[ag] *Ernest Orlando Lawrence Berkeley National Laboratory, Berkeley, CA 94720, USA*
[ah] *University of Liverpool, Liverpool L69 7ZE, United Kingdom*
[ai] *University College London, London WC1E 6BT, United Kingdom*
[aj] *Centro de Investigaciones Energeticas Medioambientales y Tecnologicas, E-28040 Madrid, Spain*
[ak] *Massachusetts Institute of Technology, Cambridge, MA 02139, USA*
[al] *Institute of Particle Physics: McGill University, Montréal, Québec, H3A 2T8 Canada*
[am] *Simon Fraser University, Burnaby, British Columbia, V5A 1S6 Canada*
[an] *University of Toronto, Toronto, Ontario, M5S 1A7 Canada*
[ao] *TRIUMF, Vancouver, British Columbia, V6T 2A3 Canada*
[ap] *University of Michigan, Ann Arbor, MI 48109, USA*
[aq] *Michigan State University, East Lansing, MI 48824, USA*
[ar] *Institution for Theoretical and Experimental Physics, ITEP, Moscow 117259, Russia*
[as] *University of New Mexico, Albuquerque, NM 87131, USA*
[at] *The Ohio State University, Columbus, OH 43210, USA*
[au] *Okayama University, Okayama 700-8530, Japan*
[av] *Osaka City University, Osaka 588, Japan*
[aw] *University of Oxford, Oxford OX1 3RH, United Kingdom*
[ax] *Istituto Nazionale di Fisica Nucleare, Sezione di Padova–Trento, Italy*
[ay] *University of Padova, I-35131 Padova, Italy*
[az] *University of Pennsylvania, Philadelphia, PA 19104, USA*
[ba] *Istituto Nazionale di Fisica Nucleare Pisa, Italy*
[bb] *University of Pisa, Italy*
[bc] *University of Siena, Italy*
[bd] *Scuola Normale Superiore, I-56127 Pisa, Italy*
[be] *University of Pittsburgh, Pittsburgh, PA 15260, USA*
[bf] *Purdue University, West Lafayette, IN 47907, USA*
[bg] *University of Rochester, Rochester, NY 14627, USA*
[bh] *The Rockefeller University, New York, NY 10065, USA*
[bi] *Istituto Nazionale di Fisica Nucleare, Sezione di Roma 1, Italy*
[bj] *Sapienza Università di Roma, I-00185 Roma, Italy*
[bk] *Rutgers University, Piscataway, NJ 08855, USA*
[bl] *Texas A&M University, College Station, TX 77843, USA*
[bm] *Istituto Nazionale di Fisica Nucleare Trieste/Udine, I-34100 Trieste, Italy*
[bn] *University of Udine, I-33100 Udine, Italy*
[bo] *University of Tsukuba, Tsukuba, Ibaraki 305, Japan*
[bp] *Tufts University, Medford, MA 02155, USA*
[bq] *University of Virginia, Charlottesville, VA 22906, USA*
[br] *Waseda University, Tokyo 169, Japan*
[bs] *Wayne State University, Detroit, MI 48201, USA*
[bt] *University of Wisconsin, Madison, WI 53706, USA*
[bu] *Yale University, New Haven, CT 06520, USA*

A R T I C L E   I N F O

A B S T R A C T

A measurement of the top quark mass (M_{top}) in the all-hadronic decay channel is presented. It uses 5.8 fb^{-1} of $p\bar{p}$ data collected with the CDF II detector at the Fermilab Tevatron Collider. Events with six to eight jets are selected by a neural network algorithm and by the requirement that at least one of the jets is tagged as a b-quark jet. The measurement is performed with a likelihood fit technique, which simultaneously determines M_{top} and the jet energy scale (JES) calibration. The fit yields a value of $M_{top} = 172.5 \pm 1.4(\text{stat}) \pm 1.0(\text{JES}) \pm 1.1(\text{syst})$ GeV/c^2.

[1] Deceased.
[2] Visitor from Istituto Nazionale di Fisica Nucleare, Sezione di Cagliari, 09042 Monserrato (Cagliari), Italy.
[3] Visitor from University of CA Irvine, Irvine, CA 92697, USA.
[4] Visitor from University of CA Santa Barbara, Santa Barbara, CA 93106, USA.
[5] Visitor from University of CA Santa Cruz, Santa Cruz, CA 95064, USA.
[6] Visitor from Institute of Physics, Academy of Sciences of the Czech Republic, Czech Republic.
[7] Visitor from CERN, CH-1211 Geneva, Switzerland.
[8] Visitor from Cornell University, Ithaca, NY 14853, USA.
[9] Visitor from University of Cyprus, Nicosia CY-1678, Cyprus.

The mass of the top quark (M_{top}) is a fundamental parameter of the standard model (SM) and its large value makes the top quark contribution dominant in loop corrections to many observables, like the W boson mass M_W. Precise measurements of M_W and M_{top} allow one to set indirect constraints on the mass of the, as yet unobserved, Higgs boson [1].

In this Letter we present a measurement of M_{top} using proton–antiproton collision events at a center-of-mass energy of 1.96 TeV. Top quarks are produced at the largest rate in pairs ($t\bar{t}$), with each top quark decaying immediately into a W boson and a b quark nearly 100% of the time [2]. In this analysis events where both the W's decay to a quark–antiquark pair ($t\bar{t} \rightarrow W^+bW^-\bar{b} \rightarrow q_1\bar{q}_2bq_3\bar{q}_4\bar{b}$) are considered. This all-hadronic final state has the largest branching ratio among the possible decay channels (46%), but it is overwhelmed by the QCD multijet background processes, which surpass $t\bar{t}$ production by three orders of magnitude even after a dedicated trigger requirement. Nevertheless, it will be shown how this difficult background can be successfully controlled and significantly suppressed with a properly optimized event selection. The fundamental analysis technique is the same exploited to obtain the previous result from CDF, and is described in details in [3]. However, improvements in the event selection and a larger dataset allow us to decrease the total uncertainty on M_{top} by 21%. The additional dataset has been acquired at higher instantaneous luminosity, which results in a higher number of background events in the data sample. Despite this fact, the introduction of significant improvements to the analysis results in the world best measurement of M_{top} in the all-hadronic channel so far, also entering with the third largest weight in the M_{top} world average calculation [4,5].

The data correspond to an integrated luminosity of 5.8 fb^{-1}. They have been collected between March 2002 and February 2010 by the CDF detector, a general-purpose apparatus designed to study $p\bar{p}$ collisions at the Tevatron and described in detail in [6]. Events used in this measurement are selected by a multijet trigger [3], and retained only if they are well contained in the detector acceptance, have no well-identified energetic electron or muon, and have a missing transverse energy[32] $\not{E}_T$ satisfying

$\not{E}_T/\sqrt{\sum E_T} < 3$ GeV$^{\frac{1}{2}}$, where $\sum E_T$ is the sum of the transverse energy E_T of all jets. Candidate events are also required to have from six to eight "tight" ($E_T \geqslant 15$ GeV and $|\eta| \leqslant 2.0$) jets. After this preselection, a total of about 5.7 M events is observed in the data, with less than 9 thousand expected from $t\bar{t}$ events. To improve the signal-to-background ratio (S/B) a b-tagging algorithm [7] is used to identify ("b-tag" or simply "tag") jets that most likely resulted from the fragmentation of a b quark. Only events with one to three tagged jets are then retained, improving the S/B by a factor of 6. In order to further increase the signal purity, a multivariate algorithm is implemented. An artificial neural network, based on a set of kinematic and jet shape variables [3], is used to take advantage of the distinctive features of signal and background events. The neural network was trained using simulated $t\bar{t}$ events generated by PYTHIA [8] and propagated through the CDF detector simulation. At this level of selection the fraction of signal events is still negligible so that the data can be used to represent the background. The value of the output node, N_{out}, is used as a discriminant between signal and background, providing a gain in S/B by an additional factor of about 30.

The background for the $t\bar{t}$ multijet final state comes mainly from QCD production of heavy-quark pairs ($b\bar{b}$ and $c\bar{c}$) and events with false tags from light-quark and gluon jets. Given the large theoretical uncertainties on the QCD multijet production cross section, the background prediction is obtained from the data themselves. The probability of tagging a jet in a background event (P^+) is evaluated using data with five tight jets and passing the preselection ($S/B \approx 1/2000$). This "tag rate" is parametrized in terms of a few relevant jet variables and is then used to estimate the probability that a candidate event belongs to the background and contains a given number of tagged jets. As described in detail in [3] this allows to predict the expected amount of background events in the selected samples as well as their distributions. For example, the average number of background 1-tag events is estimated by

$$\sum_{\text{events}} \left[\sum_{i=1}^{N_{\text{jets}}} C_{1\,\text{tag}}^i \cdot P_i^+ \prod_{k \neq i} \left(1 - P_k^+\right) \right]$$

where the outer sum runs over all events selected just before the b-tagging requirement, and the inner one over the jets of the event. The factor $C_{1\,\text{tag}}$ represents a correction to take into account correlations among jets within the same event [3], and it is parametrized as a function of the same variables used for the tag rate.

The analysis employs the template method to measure M_{top} with simultaneous calibration of the jet energy scale (JES) [3,9], allowing a strong reduction of the associated systematic uncertainty. Distributions of variables sensitive to the "true" values of M_{top} and JES, obtained by Monte Carlo (MC) events, are used as a reference ("template") in the measurement. A maximum likelihood fit is performed to define the values that best reproduce the same distributions as observed in the data. An usual choice is to consider the distributions of the event-by-event reconstructed top quark mass, m_t^{rec}, and W boson mass, m_W^{rec} as the reference templates. The JES is a multiplicative factor representing a correction applied to the raw energy of a reconstructed jet (E_T^{raw}), so that its corrected energy $E_T = \text{JES} \cdot E_T^{\text{raw}}$, is a better estimate of the energy of the underlying parton [10]. Discrepancies between data and simulation result in an uncertainty on the JES value to be applied in MC events to reproduce the data, and, as a consequence, on the

[10] Visitor from Office of Science, U.S. Department of Energy, Washington, DC 20585, USA.
[11] Visitor from University College Dublin, Dublin 4, Ireland.
[12] Visitor from ETH, 8092 Zurich, Switzerland.
[13] Visitor from University of Fukui, Fukui City, Fukui Prefecture, 910-0017 Japan.
[14] Visitor from Universidad Iberoamericana, Mexico D.F., Mexico.
[15] Visitor from University of Iowa, Iowa City, IA 52242, USA.
[16] Visitor from Kinki University, Higashi-Osaka City, 577-8502 Japan.
[17] Visitor from Kansas State University, Manhattan, KS 66506, USA.
[18] Visitor from Korea University, Seoul, 136-713, Korea.
[19] Visitor from University of Manchester, Manchester M13 9PL, United Kingdom.
[20] Visitor from Queen Mary, University of London, London, E1 4NS, United Kingdom.
[21] Visitor from University of Melbourne, Victoria 3010, Australia.
[22] Visitor from Muons, Inc., Batavia, IL 60510, USA.
[23] Visitor from Nagasaki Institute of Applied Science, Nagasaki, Japan.
[24] Visitor from National Research Nuclear University, Moscow, Russia.
[25] Visitor from Northwestern University, Evanston, IL 60208, USA.
[26] Visitor from University of Notre Dame, Notre Dame, IN 46556, USA.
[27] Visitor from Universidad de Oviedo, E-33007 Oviedo, Spain.
[28] Visitor from CNRS-IN2P3, Paris, F-75205 France.
[29] Visitor from Texas Tech University, Lubbock, TX 79609, USA.
[30] Visitor from Universidad Tecnica Federico Santa Maria, 110v Valparaiso, Chile.
[31] Visitor from Yarmouk University, Irbid 211-63, Jordan.
[32] We use a cylindrical coordinate system where θ is the polar angle with respect to the proton beam direction (z axis), ϕ is the azimuthal angle about the beam axis, and the pseudorapidity is defined as $\eta = -\ln\tan(\theta/2)$. A particle's transverse momentum p_T and transverse energy E_T are given by $|p|\sin\theta$ and $E\sin\theta$ respectively.

The missing E_T vector, $\vec{\not{E}}_T$, is defined by $\vec{\not{E}}_T = -\sum_i E_{T,i}\hat{n}_{T,i}$ where $\hat{n}_{T,i}$ is the unit vector in the x–y plane pointing from the primary interaction vertex to a given calorimeter tower i, and $E_{T,i}$ is the E_T measured in that tower. Finally $\not{E}_T = |\vec{\not{E}}_T|$.

measurements of M_{top}. Nevertheless, this value can be calibrated "in situ", using m_W^{rec} as a template. This represents a well-tested technique, first applied in [9] and now used to obtain the most precise top quark mass measurements at the Tevatron [4,5].

The templates are built as follows [3]. For each selected event, each of the six highest-E_T jets is assigned in turn to one of the six quarks of a $t\bar{t}$ all-hadronic final state. Then, for each combination the jets are arranged in two triplets (the top quarks), each including a doublet (corresponding to the W boson) and a b quark. To reduce the possible number of permutations, b-tagged jets are assigned to b quarks only, resulting in 30, 6 or 18 permutations for events with one, two or three tagged jets, respectively.[33]

For each permutation m_t^{rec} is obtained through a constrained fit based on the minimization of the following χ^2-like function:

$$\chi_t^2 = \frac{(m_{jj}^{(1)} - M_W)^2}{\Gamma_W^2} + \frac{(m_{jj}^{(2)} - M_W)^2}{\Gamma_W^2}$$
$$+ \frac{(m_{jjb}^{(1)} - m_t^{\text{rec}})^2}{\Gamma_t^2} + \frac{(m_{jjb}^{(2)} - m_t^{\text{rec}})^2}{\Gamma_t^2}$$
$$+ \sum_{i=1}^{6} \frac{(p_{T,i}^{\text{fit}} - p_{T,i}^{\text{meas}})^2}{\sigma_i^2}$$

where $m_{jj}^{(1,2)}$ are the invariant masses of the two pairs of jets assigned to light flavor quarks, $m_{jjb}^{(1,2)}$ are the invariant masses of the triplets including one pair and one jet assigned to a b quark, $M_W = 80.4$ GeV/c^2 and $\Gamma_W = 2.1$ GeV are the measured mass and natural width of the W boson [2], and $\Gamma_t = 1.5$ GeV is the assumed natural width of the top quark [11]. The jet transverse momenta are constrained in the fit to the measured values, $p_{T,i}^{\text{meas}}$, within their known resolutions, σ_i. The fit is performed with respect to m_t^{rec} and the transverse momenta of the jets $p_{T,i}^{\text{fit}}$, and, among all the permutations, the one which gives the lowest value for the minimized χ_t^2 is selected. The variable m_W^{rec} is reconstructed by the same procedure considered for m_t^{rec}, but with a χ^2 function, χ_W^2, where also the W mass is left free to vary in the fit. The selected values of m_t^{rec} and m_W^{rec} enter the respective distributions, built separately for events with exactly one or $\geqslant 2$ tags.

Signal templates are built using MC events with M_{top} values from 160 to 185 GeV/c^2, with steps of 1.0 GeV/c^2, and, for each value, moving the JES by $\Delta\text{JES} \cdot \sigma_{\text{JES}}$ from the default. Here σ_{JES} is the absolute uncertainty on the JES [10] and ΔJES is a dimensionless number. Values of ΔJES between -2 and $+2$, in steps of 0.5, have been used, and in the following we refer to this parameter to denote variations of the JES. To construct the background templates we apply the fitting technique to the data events passing the neural network selection cut, omitting the b-tagging requirement ("pretag" sample) [3]. The weight of each value of m_t^{rec} and m_W^{rec} is given by the probability of the event to belong to the background and to contain tagged jets, evaluated by the tag rates of jets, as outlined above.

Sets of simulated experiments ("pseudo-experiments", PEs) have been performed to optimize the requirements on the values of N_{out}, χ_t^2 and χ_W^2 in order to minimize the statistical uncertainty on the M_{top} measurement. As an improvement with respect to [3], two different sets of events, denoted by S_{JES} and $S_{M_{\text{top}}}$, are used to build the m_W^{rec} and m_t^{rec} templates, respectively. The set S_{JES} is selected by using cuts on N_{out} and χ_t^2, while $S_{M_{\text{top}}}$ is selected by a

---

Table 1

Selection flow for 1-tag events samples. For each requirement the number of events observed in the data, the expected number of $t\bar{t}$ signal events, the absolute efficiency on the signal (ε) and the signal-to-background ratio (S/B) are shown. For the signal $M_{\text{top}} = 172.5$ GeV/c^2 and $\Delta\text{JES} = 0$ are used. The expectations are normalized to the integrated luminosity of the data sample (5.8 fb^{-1}) using the theoretical cross section (7.46 pb), while the background is evaluated as the difference between the data and the expected signal.

Selection requirement	Data	$t\bar{t}$	ε (%)	S/B
Trigger + Presel.	5 683 210	8854	20.6	1/641
$\equiv 1$ b-tag	546 579	3861	9.0	1/141
$N_{\text{out}} > 0.97$	5743	1028	2.4	1/4.6
$\chi_W^2 < 2$ (S_{JES})	4368	881	2.1	1/4.0
$\chi_t^2 < 3$ ($S_{M_{\text{top}}}$)	2256	604	1.4	1/2.7

Table 2

Selection flow for $\geqslant 2$-tag events samples. The same notations of Table 1 are used.

Selection requirement	Data	$t\bar{t}$	ε (%)	S/B
Trigger + Presel.	5 683 210	8854	20.6	1/641
$\geqslant 2$ b-tags	47 229	1520	3.5	1/30
$N_{\text{out}} > 0.94$	2379	740	1.7	1/2.2
$\chi_W^2 < 3$ (S_{JES})	1196	468	1.1	1/1.6
$\chi_t^2 < 4$ ($S_{M_{\text{top}}}$)	600	316	0.7	1/0.9

further requirement on χ_t^2, so that $S_{M_{\text{top}}}$ corresponds to a subset of S_{JES}. This new procedure contributes in reducing the final total uncertainty on M_{top} with respect to [3] by about 12%. Tables 1 and 2 report the flow of the event selection for 1-tag and $\geqslant 2$-tag events, respectively. As the final requirements are optimized separately for the two tagging categories, the b-tag requirement is included in the flow just after the preselection.

In order to measure M_{top} with the simultaneous calibration of the JES, a fit is performed in which an unbinned extended likelihood function is maximized to find the values of M_{top}, ΔJES, the number of signal (n_s) and background (n_b) events for each tagging category which best reproduce the observed distributions of m_t^{rec} and m_W^{rec} [3]. The likelihood depends on the probability density functions (p.d.f.'s) of m_t^{rec} and m_W^{rec} expected for signal (s) and background (b), $P_s(m_t^{\text{rec}}|M_{\text{top}}, \Delta\text{JES})$, $P_s(m_W^{\text{rec}}|M_{\text{top}}, \Delta\text{JES})$, $P_b(m_t^{\text{rec}})$, and $P_b(m_W^{\text{rec}})$. The notation points out that the shapes of the signal p.d.f.'s are functions of the fit parameters M_{top} and ΔJES. This dependence is obtained by fitting the whole set of templates, initially built as histograms. Fig. 1 shows examples of signal and background templates for the $\geqslant 2$-tag sample, with the corresponding p.d.f.'s superimposed.

The presence of the different sets S_{JES} and $S_{M_{\text{top}}}$ requires the generalizations of some of the terms of the likelihood with respect to [3]. The function can be divided into three parts:

$$\mathcal{L} = \mathcal{L}_{1\,\text{tag}} \times \mathcal{L}_{\geqslant 2\,\text{tags}} \times \mathcal{L}_{\Delta\text{JES}_{\text{constr}}}$$

where $\mathcal{L}_{\Delta\text{JES}_{\text{constr}}}$ is a Gaussian term constraining the JES to the nominal value (i.e. ΔJES to 0) within its uncertainty:

$$\mathcal{L}_{\Delta\text{JES}_{\text{constr}}} = e^{-\frac{(\text{JES} - \text{JES}_{\text{constr}})^2}{2\sigma_{\text{JES}}^2}}$$
$$= e^{-\frac{[(\text{JES}_{\text{constr}} + \Delta\text{JES} \cdot \sigma_{\text{JES}}) - \text{JES}_{\text{constr}}]^2}{2\sigma_{\text{JES}}^2}}$$
$$= e^{-\frac{[\Delta\text{JES}]^2}{2}}.$$

Terms $\mathcal{L}_{1\,\text{tag}}$ and $\mathcal{L}_{\geqslant 2\,\text{tags}}$ are in turn defined as:

$$\mathcal{L}_{1, \geqslant 2\,\text{tags}} = \mathcal{L}_{\Delta\text{JES}} \times \mathcal{L}_{M_{\text{top}}} \times \mathcal{L}_{\text{evts}} \times \mathcal{L}_{N_{\text{constr}}^{\text{bkg}}},$$

where, omitting the dependences on M_{top} and Δ_{JES},

---

[33] If three b-tagged jets are present in the event, the three possible assignments of two out of three of them to b quarks are also considered, while the remaining one is treated as a light flavor jet.
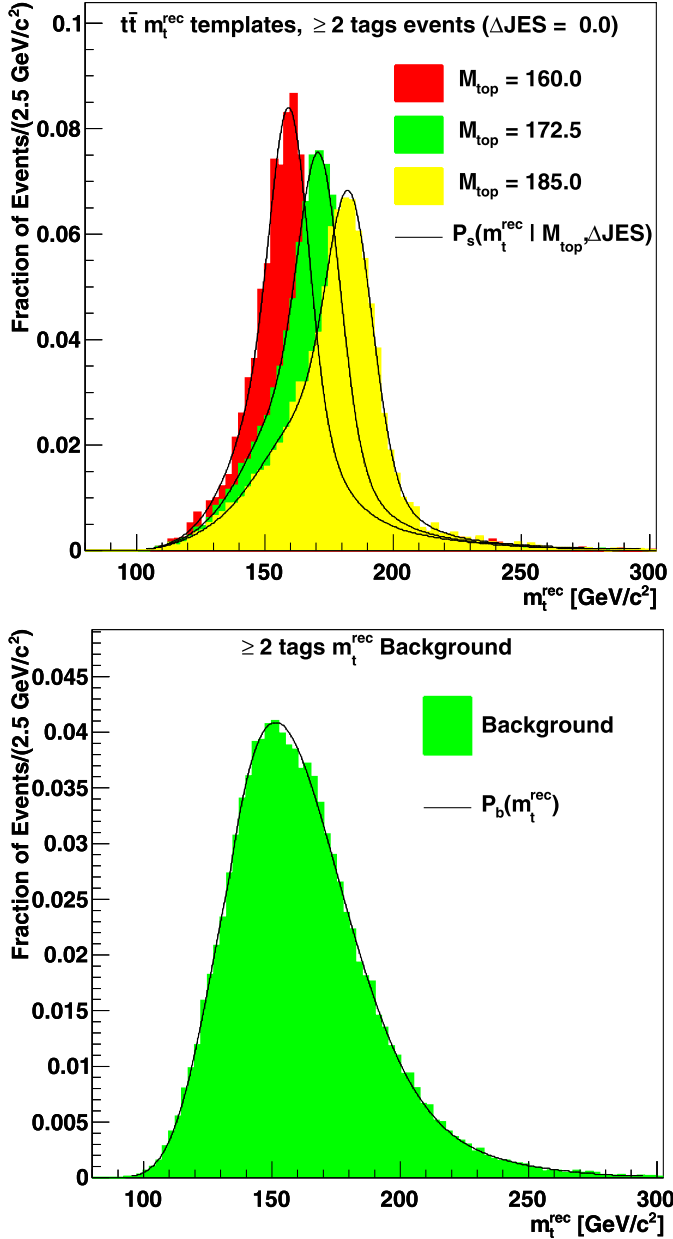
Fig. 1. Templates of m_t^{rec} for events with $\geqslant 2$ tags and corresponding probability density functions superimposed. Top plot: the signal p.d.f., P_s, for various values of M_{top} and ΔJES $= 0$. Bottom plot: the background p.d.f., P_b.

$$\mathcal{L}_{\Delta JES} = \prod_{i=1}^{N_{obs}^{S_{JES}}} \frac{n_s P_s^{m_W^{rec}}(m_{W,i}) + n_b P_b^{m_W^{rec}}(m_{W,i})}{n_s + n_b},$$

$$\mathcal{L}_{M_{top}} = \prod_{i=1}^{N_{obs}^{S_{M_{top}}}} \frac{\mathcal{A}_s n_s P_s^{m_t^{rec}}(m_{t,i}) + \mathcal{A}_b n_b P_b^{m_t^{rec}}(m_{t,i})}{\mathcal{A}_s n_s + \mathcal{A}_b n_b},$$

$$\mathcal{L}_{evts} = \sum_{r_s + r_b = N_{obs}^{S_{JES}}} P(r_s, n_s) \cdot P(r_b, n_b)$$

$$\cdot \left[\sum_{\substack{t_s \leqslant r_s, t_b \leqslant r_b \\ t_s + t_b = N_{obs}^{S_{M_{top}}}}} B(t_s, r_s, \mathcal{A}_s) \cdot B(t_b, r_b, \mathcal{A}_b) \right]$$

and

$$\mathcal{L}_{N_{constr}^{bkg}} = e^{-\frac{[n_b - n_{(b,exp)}]^2}{2\sigma_{n_{(b,exp)}}^2}}.$$

In the first term the probability to observe the set $m_{W,i}$ ($i = 1, \ldots, N_{obs}^{S_{JES}}$) of m_W^{rec} values reconstructed in the data is calculated by the signal and background expected distributions, $P_s^{m_W^{rec}}$ and $P_b^{m_W^{rec}}$ respectively, as a function of the free parameters of the fit M_{top}, ΔJES, n_s, and n_b. In the second the same is done for the distributions of the observed reconstructed top masses, $m_{t,i}$ ($i = 1, \ldots, N_{obs}^{S_{M_{top}}}$), and the m_t^{rec} probability density functions. The factors $\mathcal{A}_s(M_{top}, \Delta JES)$ and $\mathcal{A}_b$ represent the acceptance of $S_{M_{top}}$ with respect to S_{JES} for signal and background, respectively (i.e., the fraction of events selected by the requirements on χ_t^2 only). For the signal this acceptance is parametrized as a function of the fit parameters M_{top} and ΔJES. The third term, $\mathcal{L}_{evts}$, gives the probability to observe simultaneously the number of events selected in the data in the S_{JES} and the $S_{M_{top}}$ samples, given the assumed values for the average number of signal (n_s) and background (n_b) events to be expected in S_{JES} and the acceptances $\mathcal{A}_s(M_{top}, \Delta JES)$ and $\mathcal{A}_b$. It depends on the Poisson (P) and Binomial (B) probabilities

$$P(r, n) = \frac{e^{-n} \cdot n^r}{r!},$$

$$B(t, r, \mathcal{A}) = \binom{r}{t} \cdot \mathcal{A}^t \cdot (1 - \mathcal{A})^{r-t}.$$

In the last term, $\mathcal{L}_{N_{constr}^{bkg}}$, the parameter n_b is constrained by a Gaussian to the *a priori* background estimate i.e. $n_{(b,exp)} = 3652 \pm 181$ for 1-tag events and $n_{(b,exp)} = 718 \pm 14$ for $\geqslant 2$-tag events.

The possible presence of biases in the values returned by the likelihood fit has been investigated. Pseudo-experiments are performed assuming specific values for M_{top} and ΔJES and "pseudo-data" are therefore extracted from the corresponding signal and background templates. The results of these PEs have been compared to the input values, and calibration functions to be applied to the output from the fit have been defined in order to obtain, on average, a more reliable estimate of the true values and uncertainties.

Finally, the likelihood fit is applied to data. After the event selection described above, we are left with 4368 and 1196 events with one and $\geqslant 2$ tags (147 have 3 tags), respectively, in the S_{JES} sample. The corresponding expected backgrounds amount to 3652 ± 181 and 718 ± 14 events, respectively. The tighter requirements used for the $S_{M_{top}}$ samples select 2256 with one tag and 600 with $\geqslant 2$ tags (76 have 3 tags), with average background estimates of 1712 ± 77 and 305 ± 22 events, respectively.

For these events the variables m_W^{rec} and m_t^{rec} have been reconstructed and used as the data inputs to the likelihood fit. Once the calibration procedure has been applied, the measurements of M_{top} and ΔJES are

$$M_{top} = 172.5 \pm 1.4(stat) \pm 1.0(JES)\ GeV/c^2,$$

$$\Delta JES = -0.1 \pm 0.3(stat) \pm 0.3(M_{top}).$$

Fig. 2 shows the measured values together with the negative log-likelihood contours whose projections correspond to one, two, and three σ uncertainties on the values of M_{top} and ΔJES as obtained from the likelihood fit.

Fig. 3 shows the m_t^{rec} and m_W^{rec} distributions for the data compared to the expected background and the signal for M_{top} and
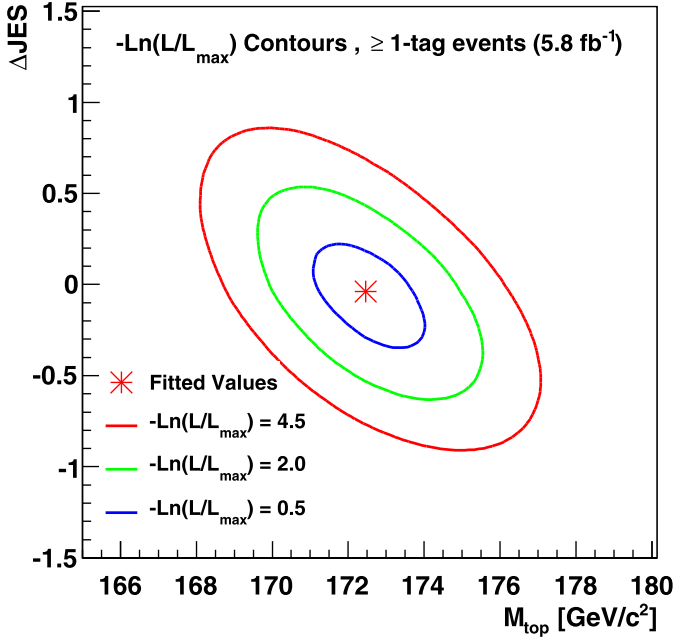
Fig. 2. Negative log-likelihood contours for the likelihood fit performed for the M_{top} and ΔJES measurement. The minimum is shown along with the contours whose projections correspond to one, two, and three σ uncertainties on the M_{top} and ΔJES measurements.

Table 3
Sources of systematic uncertainty affecting the M_{top} and ΔJES measurements. The total uncertainty is obtained by the quadrature sum of each contribution.

Source	δM_{top} (GeV/c^2)	$\delta \Delta$JES
Residual bias	0.2	0.03
Calibration	0.1	0.01
Generator	0.5	0.21
Initial/final state radiation	0.1	0.04
b-jet energy scale	0.2	0.05
b-tag	0.1	0.01
Residual JES	0.4	–
Parton distribution functions	0.2	0.04
Multiple $p\bar{p}$ interactions	0.1	0.04
Color reconnection	0.3	0.12
Statistics of templates	0.3	0.05
Background	0.6	0.11
Trigger	0.2	0.04
Total	1.1	0.29

ΔJES corresponding to the measured values. The signal and background distributions are normalized to the respective yields as fitted to the data, with the 1-tag and $\geqslant$ 2-tag contributions summed together.

Various sources of systematic uncertainties affect the M_{top} and ΔJES measurements, as described in [3]. They are evaluated by performing PEs using templates built by signal samples where effects due to systematic uncertainties have been included. The differences in the average values of M_{top} and ΔJES with respect to the PEs performed with default templates are then taken into account. Possible residual biases existing after the calibration, and uncertainties on the parameters of the calibration functions are also taken into account. The largest contributions come from uncertainties on the modeling of the background, on the simulation of $t\bar{t}$ events, and on the individual corrections which JES depends on [10]. Table 3 shows a summary of all the systematic uncertainties.
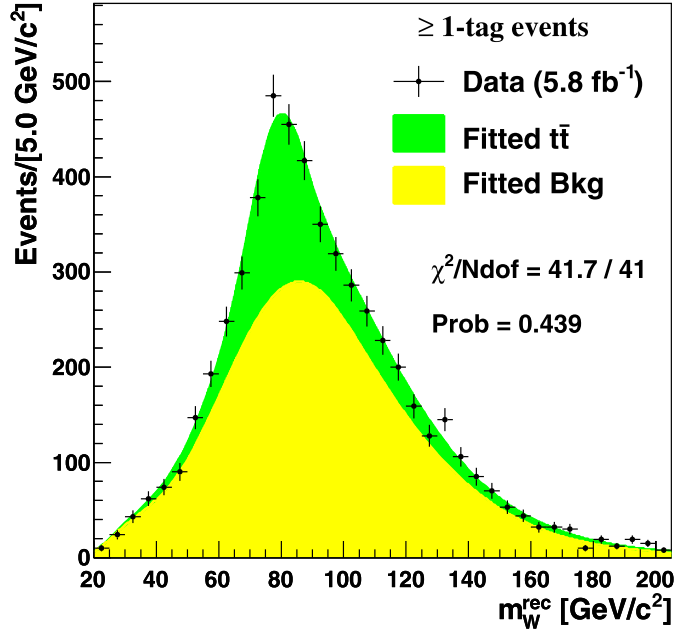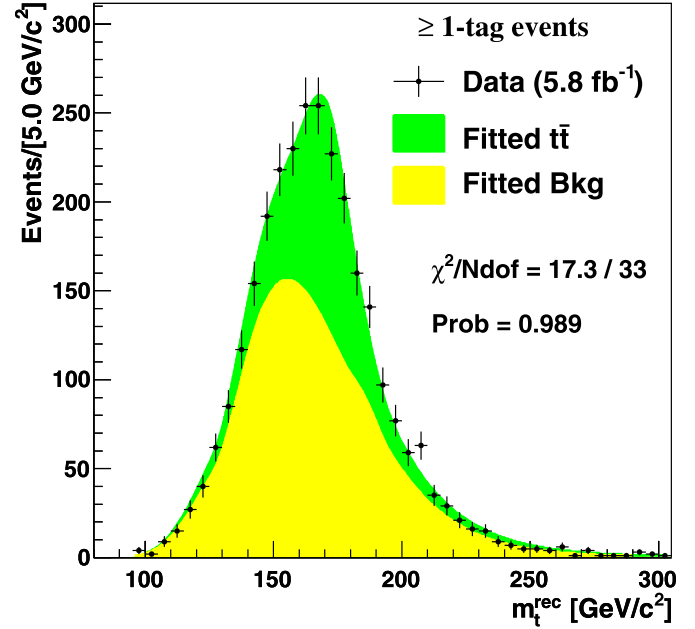

Fig. 3. Distributions of m_t^{rec} (top plot) and m_W^{rec} (bottom plot) as obtained in the selected data (black points) with $\geqslant$ 1 tag, compared to the distributions from signal and background corresponding to the measured values of M_{top} and ΔJES. The expected distributions are normalized to the best fit yields.

In summary, we have presented a measurement of the top quark mass in the all-hadronic channel, using $p\bar{p}$ collision data corresponding to an integrated luminosity of 5.8 fb^{-1}. An optimized event selection, based mainly on a neural network and a b-tagging algorithm, allows us to select candidate event samples with S/B close to 1 in spite of the huge background still existing at trigger level. The simultaneous calibration of the jet energy scale, following a well-established technique, allows to reduce down to 1 GeV/c^2 the systematic uncertainty due to this source. The value obtained for the JES is in agreement both with the default value [10] and with the results obtained by other measurements of the top quark mass performed by the CDF Collaboration using the *in situ* calibration technique [4,5]. The measured value of the top quark mass is

$M_{\text{top}} = 172.5 \pm 1.4(\text{stat}) \pm 1.0(\text{JES}) \pm 1.1(\text{syst})$ GeV/c^2, with a total uncertainty of 2.0 GeV/c^2. This result complements and is consistent with the most recent measurements obtained in other channels by the CDF and D0 Collaborations, and also represents the most accurate all-hadronic measurement at the Tevatron so far.

Acknowledgements

References

[1] ALEPH Collaboration, CDF Collaboration, D0 Collaboration, DELPHI Collaboration, L3 Collaboration, OPAL Collaboration, SLD Collaboration, LEP Electroweak Working Group, Tevatron Electroweak Working Group, SLD Electroweak and Heavy Flavour Groups, Precision electroweak measurements and constraints on the standard model, arXiv:1012.2367, 2010.
[2] K. Nakamura, et al., Particle Data Group, J. Phys. G 37 (2010) 075021.
[3] T. Aaltonen, et al., CDF Collaboration, Phys. Rev. D 81 (2010) 052011.
[4] A. Barbaro Galtieri, F. Margaroli, I. Volobouev, Rept. Prog. Phys. 75 (2012) 056201.
[5] Tevatron Electroweak Working Group, D0 Collaborations, Combination of CDF and D0 results on the mass of the top quark using up to 5.8 fb^{-1} of data, arXiv:1107.5255 [hep-ex], 2011.
[6] D. Acosta, et al., CDF Collaboration, Phys. Rev. D 71 (2005) 032001.
[7] D. Acosta, et al., CDF Collaboration, Phys. Rev. D 71 (2005) 052003.
[8] T. Sjöstrand, et al., Comput. Phys. Commun. 135 (2001) 238.
[9] A. Abulencia, et al., CDF Collaboration, Phys. Rev. D 73 (2006) 032003.
[10] A. Bhatti, et al., Nucl. Instrum. Methods Phys. Res., Sect. A 566 (2006) 375.
[11] S.M. Oliveira, L. Brucher, R. Santos, A. Barroso, Phys. Rev. D 64 (2001) 017301.